Soils and Foundations ▮▮▮▮;▮(▮):▮▮▮–▮▮▮

HOSTED BY

The Japanese Geotechnical Society

Soils and Foundations

www.sciencedirect.com
journal homepage: www.elsevier.com/locate/sandf

Cyclic resistance of two unsaturated silty sands against soil liquefaction

Yoshimichi Tsukamoto[a,*], Shohei Kawabe[b], Jo Matsumoto[c], Shotaro Hagiwara[a]

[a]*Department of Civil Engineering, Tokyo University of Science, Japan*
[b]*National Agriculture and Food Research Organization, Japan*
[c]*Tokyu Construction Co., Ltd., Japan (Formerly graduate student, Department of Civil Engineering, Tokyo University of Science, Japan)*

Received 20 September 2013; received in revised form 28 July 2014; accepted 14 August 2014

Abstract

The changes of the cyclic resistance of two silty sands under unsaturated, partially saturated and fully saturated conditions are examined based on a series of undrained cyclic tests conducted using triaxial test apparatus specially equipped for testing unsaturated soils as well as ordinary triaxial test apparatus for testing partially saturated and fully saturated soils. Based on the observations of volumetric strain, pore air and pore water pressures of unsaturated soil specimens, the possibility of soil liquefaction triggering under different degrees of saturation is examined and discussed. The changes in the cyclic resistance under different degrees of saturation are then examined. Those two unsaturated silty sands with different grain size compositions are found to give rise to different responses on the volumetric strain as well as pore air and pore water pressure developments during undrained cyclic loading, leading to different relations between cyclic resistance and degree of saturation, covering unsaturated, partially saturated and fully saturated conditions.

Keywords: Unsaturated soil; Cyclic resistance; Silty sand; Soil liquefaction (IGC: D3/D7)

1. Introduction

In evaluating the possibility of soil liquefaction triggering during earthquakes, any soil layers located above a groundwater table are generally assumed as non-liquefiable. Located above a groundwater table are unsaturated soil layers, where field measurements using tensiometers revealed that negative pore water pressures were observed in many geotechnical engineering applications, (Fredlund and Rahardjo, 1993 and others).

It is also known that partially saturated soil layers containing some minute air bubbles are located down to approximately 5 m below a groundwater table. This is evident from the results of velocity logging tests that the velocity of primary wave propagation frequently stays at around $V_p = 500$ to 1000 m/sec at such soil layers, which is well below the value of $V_p = 1600$ m/sec for fully saturated conditions. The liquefaction resistance and undrained shear strength of partially saturated sands have been well examined, (Tsukamoto et al., 2002, Yang, 2002, Ishihara and Tsukamoto, 2004, Ishihara et al., 2004, Yang, 2004, Kamata et al., 2009, and others).

The most recent research efforts on the liquefaction of saturated sands include the effects of initial static shear applications on the subsequent liquefaction accompanying large deformation of soils, (Chiaro et al., 2012, 2013). With respect to mechanics of unsaturated soil behaviour, Higo et al. (2013) had a close look at localized deformation developed within partially saturated sand subjected to triaxial compression, by using microfocus X-ray CT with digital image correlation.

*Correspondence to: Department of Civil Engineering, Tokyo University of Science, 2641, Yamazaki, Noda, Chiba 278–8510 Japan.
E-mail address: ytsoil@rs.noda.tus.ac.jp (Y. Tsukamoto).
Peer review under responsibility of The Japanese Geotechnical Society.

http://dx.doi.org/10.1016/j.sandf.2014.11.005
0038-0806/

Nomenclature

e	void ratio
p	mean stress, $=(\sigma_a+2\sigma_o)/3$
q	deviator stress, $=\sigma_a-\sigma_o$
r_n	stress reduction ratio, $=\sigma_n$ / σ_{no}
r_{n5}	stress reduction ratio observed at DA$\varepsilon_a=5\%$
u_a	pore air pressure
u_{ao}	initial pore air pressure defined in gauge pressure
u_{ao_abs}	initial pore air pressure defined in absolute pressure
u_w	pore water pressure
B_a	pore air pressure coefficient
B_w	pore water pressure coefficient
D_r	relative density
N_c	number of cycles in undrained cyclic triaxial tests
S_r	degree of saturation
S_{ri}	initial degree of saturation
S_u	matric suction
S_{uo}	initial matric suction
S_{u5}	matric suction observed at DA$\varepsilon_a=5\%$
V_{ao}	initial volume of pore air
ΔV_a	change of volume of unsaturated soil structure
ε_a	axial strain
ε_h	lateral strain
ε_v	volumetric strain
ε_{v5}	volumetric strain observed at DA$\varepsilon_a=5\%$
$\varepsilon_{v,a}$	limiting pore-air diminishing volumetric strain
$\varepsilon_{v,l}$	limiting liquefaction-triggering volumetric strain
γ	shear strain
σ_a	axial stress
σ_d	single amplitude of cyclic axial stress
σ_n	net stress
σ_{no}	initial net stress
σ_o	confining stress (cell pressure)
σ'_o	effective confining stress
σ_{o_abs}	confining stress defined in absolute pressure

Ishikawa et al. (2014) introduced a newly developed medium-size triaxial apparatus using a pressure membrane method that enables installations of water supply and drainage paths on both sides of soil specimens. It proved to be effective in reducing testing time for unsaturated soil specimens.

The liquefaction resistance of unsaturated sand has also drawn attention recently and was examined in detail by Unno et al. (2008). In their study, the possibility of soil liquefaction triggering in unsaturated clean fine sand was discussed in relation to the developments of pore air and pore water pressures as well as volumetric strain, and it was concluded that even when the degree of saturation is small, the pore air and pore water pressures develop to become equal to the initial confining stress during cyclic loading, which they defined as the occurrence of soil liquefaction in unsaturated soils. In addition, following 2011 off the Pacific coast of Tohoku Earthquake, ground improvements such as lowering of groundwater tables and injection of air bubbles have been suggested as a way to counter soil liquefaction, especially in residential developments. Therefore, more research efforts need to be devoted towards exploring the liquefaction resistance of unsaturated soils. The aim of the present study is to examine the cyclic resistance of two silty sands with different grain compositions under unsaturated, partially saturated and fully saturated conditions by conducting multiple series of undrained cyclic triaxial tests.

2. Saturation in soils

In this study, the soil conditions are described using the terminology "unsaturated", "partially saturated" and "fully saturated". Apart from these ordinary categories describing the degree of saturation, another category, "gassy sands", has been introduced for marine deposits, (Grozic et al., 1999, 2000). The distinction of unsaturated and saturated conditions was illustrated by Fredlund and Rahardjo (1993). The distinctions of "unsaturated", "partially saturated" and "fully saturated" conditions can be made as shown in Fig. 1. In Fig. 1, the distributions of pore air and pore water pressure with depth are shown. At a soil layer located well above a groundwater table, large matric suction comes into effect due to the surface tension developed at the pore air and pore water interfaces within soil structures, where matric suction S_u is defined as the difference between the pore air and pore water pressures, $S_u=u_a-u_w$. The surface tension tends to interact with soil structures, and this affects the mobilisation of shear strength. In this unsaturated soil layer, there are some continuous air phases within soil structures. With increasing depth, as the soil undergoes some increase in the confining stress σ_o, the pore air and pore water pressures also increases. The rates of such increases are defined by the pore pressure coefficients, $B_a=du_a/d\sigma_o$ and $B_w=du_w/d\sigma_o$. In the absence of soil aggregates, these coefficients are equal to 1. However, in the presence of soil aggregates, these coefficients are lower than 1 due to the surface tension. The pore water pressure tends to increase faster than the pore air pressure in response to the increase in the confining stress, and the matric suction gradually reduces. The continuous air phases within soil structures consequently tend to diminish, and instead the occluded air bubbles become predominant. This transition is most likely to occur above a groundwater table, when the air entry value of the soil is met along the relation between matric suction and degree of saturation. While the occluded air bubbles do not interact with soil structure, they do affect the compressibility of pore fluids. At some point the matric suction becomes negligible, which makes the two pore pressure coefficients equal as $B_a \approx B_w$. However, the pore water pressure coefficient B_w is lower than 1 due to the presence of occluded air bubbles. This assumption is impractical for silts and clays, but is fairly reasonable for sands. The pore water

Please cite this article as: Tsukamoto, Y., et al., Cyclic resistance of two unsaturated silty sands against soil liquefaction. Soils and Foundations (2014), http://dx.doi.org/10.1016/j.sandf.2014.11.005

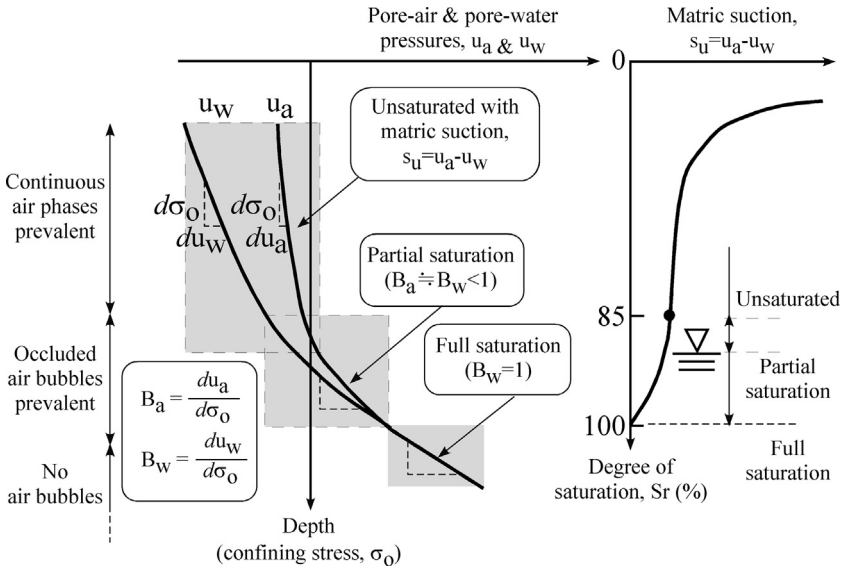

Fig. 1. Schematic interpretation of fully, partially and unsaturated soil deposits.

pressure coefficient eventually becomes equal to 1 at full saturation, i.e., $B_w=1$.

3. Testing details

3.1. Testing apparatus and procedure for unsaturated soils

In conventional triaxial tests for saturated soils, the effective stress state is given as σ_o-u_w, and the cell pressure σ_o and pore water pressure u_w (back pressure) are controlled separately. However, in determining the stress state in unsaturated soils, two components of stress state variables are necessary, (Fredlund and Rahardjo, 1993). They are the net normal stress, $\sigma_n=\sigma_o-u_a$, and matric suction, u_a-u_w. In order to provide independent controls on these two stress state variables, the cell pressure σ_o, pore air pressure u_a and pore water pressure u_w need to be regulated and monitored separately. In so doing, the triaxial testing apparatus and method for unsaturated soils have been well established ever since the filtering techniques for pore water and air intrusions were invented using ceramic disks and glass fibre filters. In the present study, the same technique is used in controlling the pore water and pore air pressures independently, as shown in Fig. 2. A water-saturated ceramic disk with an air entry value of 100 kPa is mounted in the pedestal located at the bottom of soil specimens, and a couple of glass fibre filters are placed to cover the surface of small porous stones in the cap located at the top of soil specimens. The pore water pressure, u_w, is therefore applied from the bottom of soil specimens through a pore water tube, and monitored by a pore water pressure transducer placed along the pore water tube. The pore air pressure, u_a, is applied from the top of soil specimens through a pore air tube, and monitored by a pore air pressure transducer embedded within the cap. A solenoid valve is introduced along the pore air tube and placed next to the pore air pressure transducer. When the "pore air-undrained" condition is imposed to soil specimens,

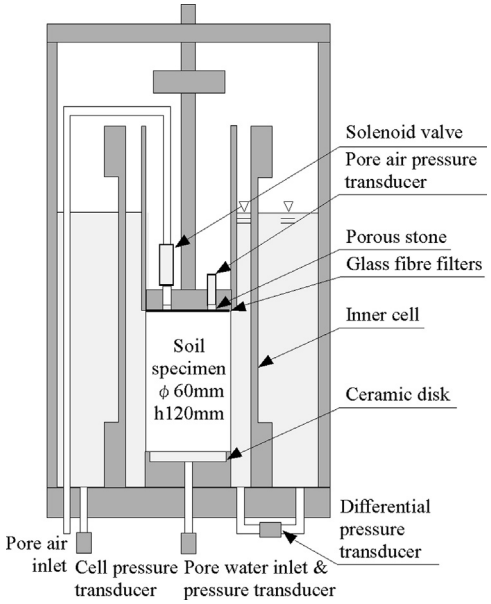

Fig. 2. Testing apparatus.

this solenoid valve is remotely closed to make the pore air tube connected to the top of soil specimens as short as possible, thus eliminating the effects of compressible air within a tube on the response of pore air pressure itself.

Another aspect of unsaturated soil testing techniques is the measurement of volume changes of unsaturated soil specimens occurring during shearing, since unsaturated soil specimens containing compressible pore air can cause substantial volume changes during shearing, even when the undrained condition for pore water as well as pore air is imposed. In the present study, the combination of an inner cell and a differential pressure transducer is introduced to monitor the volume change of a soil specimen placed inside the inner cell. The use of an inner cell and a differential pressure transducer has been adopted for unsaturated triaxial tests by Sawada et al.

Please cite this article as: Tsukamoto, Y., et al., Cyclic resistance of two unsaturated silty sands against soil liquefaction. Soils and Foundations (2014), http://dx.doi.org/10.1016/j.sandf.2014.11.005

(2006) and Unno et al. (2008). When any volume change of a soil specimen occurs, the water level inside the inner cell changes accordingly, while the water level of an outer cell remains the same. The difference in the water levels of the inner and outer cells is then monitored by a differential pressure transducer, which can be converted to the volume change of a soil specimen.

There can be two ways in conducting undrained triaxial tests on unsaturated soils. One is to shut the valve for pore water and to leave the valve for pore air open, corresponding to the "pore water-undrained and pore air-drained" condition. This kind of triaxial compression tests was conducted previously by Kamata et al. (2007), and their finding was that the matric suction can be reduced during triaxial compression, though the effective stress, $\sigma_o - u_w$, does not reduce since the level of pore water pressure cannot exceed that of pore air pressure. Another way in conducting undrained triaxial tests on unsaturated soils is to shut both of the valves for pore water and pore air, corresponding to the "pore water-undrained and pore air-undrained" condition. In the present study, multiple series of cyclic triaxial tests are conducted under the "pore water-undrained and pore air-undrained" condition.

The testing procedure consists of preparation of soil specimens, drained isotropic consolidation, and undrained cyclic tests. The triaxial soil specimens of 60 mm in diameter and 120 mm in height are prepared by the method of wet tamping. Upon assembling the cap and pedestal to soil specimens and making the inner and outer cells filled with water, the valve for pore water is closed and the valve for pore air is left opened. The cell pressure σ_o is then gradually increased and maintained at $\sigma_o = 50$ kPa, leaving the pore water undrained and the pore air drained at an atmospheric pressure, ($u_a = 0$) during the cell pressure application. The initial matric suction S_{uo} is slowly induced during the course of the above process. By remotely closing the solenoid valve for pore air, the undrained condition for pore air is imposed. Since both of the valves for pore water and pore air are closed, the "pore water-undrained and pore air-undrained" condition is established, and cyclic stress is axially applied to soil specimens. The frequency of cyclic loading needs to be determined from various points of view. It needs to be slow enough to ensure the accuracy of measurements and also to allow any equilibrium among soil particles, pore water and pore air within unsaturated soils. However, it also needs to be fast enough to replicate field seismic events. In the present study, the frequency of cyclic loading is chosen as 0.05 Hz.

3.2. Soil samples and test series

Two soil materials are used in the present study, Inagi sand and Urayasu sand. Inagi sand is a silty sand with non-plastic fines, and was retrieved from the site of residential development in Inagi city. Urayasu sand is also a silty sand with non-plastic fines, and was retrieved as a sand boil at one of the liquefied areas in Urayasu city during 2011 Great East Japan Earthquake. The physical properties and grain size distributions of the soils are shown in Table 1 and Fig. 3. In the present study, the densities of soil specimens are characterised by means of relative density D_r, where the minimum and maximum void ratios were determined by the methods stipulated by Japanese Geotechnical Society (2009), though the use of JGS methods is restricted to the soils containing 5% or less fines of less than 0.075 mm in particle diameter.

Table 1
Physical properties of soils.

Soil	Inagi sand	Urayasu sand
Specific gravity, ρ_s (g/cm^3)	2.73	2.71
Maximum void ratio, e_{max}	1.803	1.450
Minimum void ratio, e_{min}	1.023	0.850
Fines content, F_c (%)	26.7	40.2
D_{10} (mm)	0.006	0.027

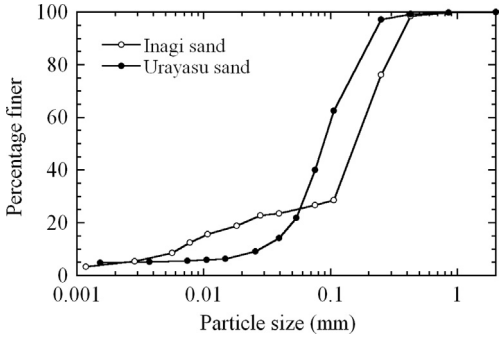

Fig. 3. Grain size distributions of soils.

Table 2
Test series under unsaturated conditions.

Soil	D_r (%)	S_r (%)	Confining stress, σ_o (kPa)	Initial net stress, σ_{no} ($=\sigma_o - u_a$) (kPa)
Inagi sand	100–103	48, 55, 67	50	50
	90–95	44, 50, 69		
	80	41, 48		
Urayasu sand	52	51		
	68–70	46, 60, 67		
	60–63	43, 56, 69		

By using these two soil samples, unsaturated soil specimens with different values of relative density D_r and degree of saturation S_r are prepared, and multiple series of cyclic tests are conducted under the "pore water-undrained and pore air-undrained" condition, as shown in Table 2. It was intended to produce soil specimens as loose as possible. However, it was very difficult to produce soil specimens with relative density lower than those shown in Table 2 from such fines-containing sands.

In addition to the test series on unsaturated soil specimens as described above, additional series of undrained cyclic tests were conducted on partially and fully saturated soil specimens by using an ordinary triaxial test apparatus, as shown in Table 3. All the tests were carried out on soil specimens prepared by the method of wet tamping and isotropically consolidated to an effective confining stress of $\sigma'_o = 100$ kPa. In Table 3, there are two methods denoted as "p-constant" and

Please cite this article as: Tsukamoto, Y., et al., Cyclic resistance of two unsaturated silty sands against soil liquefaction. Soils and Foundations (2014), http://dx.doi.org/10.1016/j.sandf.2014.11.005

Table 3
Test series under partially and fully saturated conditions.

Soil	Type of tests	D_r (%)	B-value	Initial effective confining stress, σ'_o (kPa)
Inagi sand	Partially saturated (p-constant)	100–104	0.04–0.05	100
		78–80		
	Fully saturated	116–122	> 0.95	
		102–104		
		78–80		
Urayasu sand	Partially saturated (σ_o-constant)	70	0.8	
		60		
	Fully saturated	70–80	> 0.95	
		60		

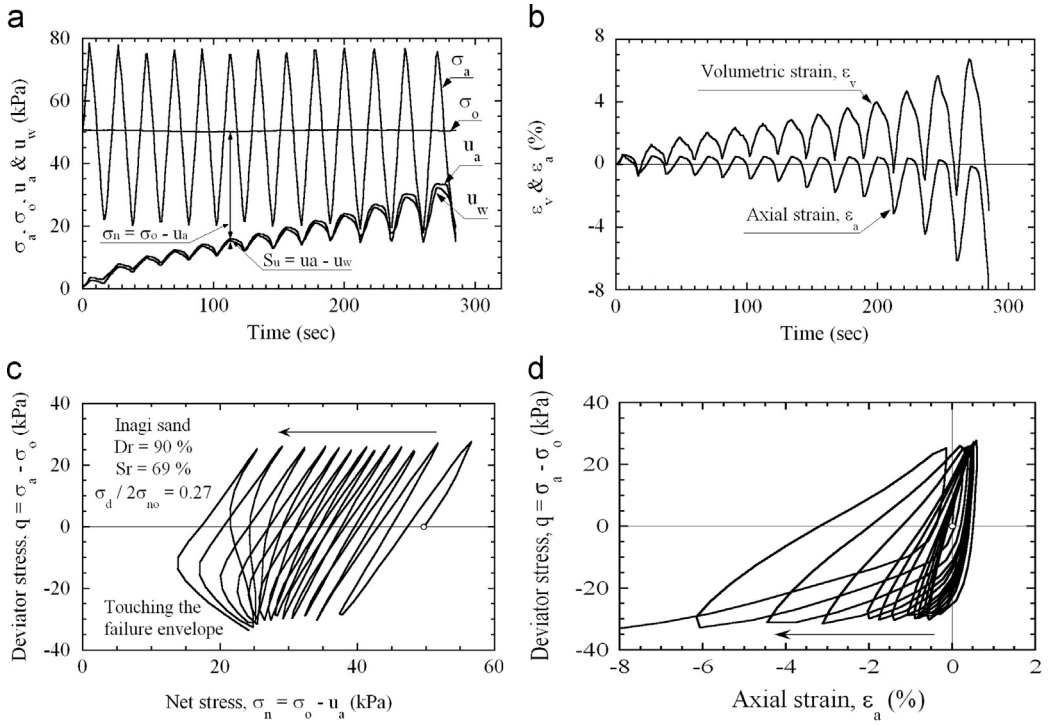

Fig. 4. Typical test results, (a) σ_a, σ_o, u_a & u_w – time, (b) ε_v & ε_a – time, (c) $q-\sigma_n$, (d) $q-\varepsilon_a$, (Inagi sand, D_r=90%, S_r=69%, σ_d / 2σ_{no}=0.28).

"σ_o-constant" for conducting undrained cyclic triaxial tests on partially saturated sands. The advantages and procedure for conducting "p-constant" tests on partially saturated soils were demonstrated by Tsukamoto et al. (2002), where the value of mean stress p is kept constant during undrained cyclic loading by adjusting the confining stress σ_o in accordance with the change in the axial stress σ_a. On the other hand, the confining stress σ_o is kept constant during undrained cyclic loading in the "σ_o-constant" tests. The use of these two methods only stems from availability of testing equipments, and is not intended to examine its consequence. Those tests are conducted to obtain good estimates of cyclic resistance of partially saturated sands, in order to make comparisons with those of unsaturated sands. The cyclic resistance and undrained shear strength of partially saturated sands have recently been examined in the past studies, including Tsukamoto et al. (2002), Ishihara and Tsukamoto (2004), Ishihara et al. (2004), Kamata et al. (2009) and others. The pore water pressure coefficient of B-value is used to control the partial saturation of soil specimens. Since the relation of B-value and S_r has been well investigated theoretically as well as experimentally, the value of S_r for each of the tests is estimated.

4. Test results

4.1. Typical test results

Fig. 4 shows one of the test results on Inagi sand with D_r=90% and S_r=69% under the cyclic stress ratio of σ_d/(2σ_{no})=0.27, where σ_d is the single amplitude of cyclic stress and σ_{no} is the initial net stress achieved after drained isotropic consolidation, i.e. σ_{no}=50 kPa. The plots of time history of axial stress σ_a, confining stress σ_o, pore air pressure u_a and pore water pressure u_w are shown in Fig. 4(a). The pore air pressure

u_a and pore water pressure u_w are responded to increase during undrained cyclic excitation. The major change was found to be in the net stress, $\sigma_n=\sigma_o-u_a$, and was observed as a gradual reduction, whereas only a minor change was noted in the matric suction, $S_u=u_a-u_w$. The plots of time history of volumetric strain ε_v and axial strain ε_a are shown in Fig. 4 (b). Significant volume contraction occurs during undrained cyclic excitation, with the cyclic amplitude of axial strain gradually increasing and eventually deviating towards extension at a later stage of the test. The stress path is indicated in the plots of net stress, $\sigma_n=\sigma_o-u_a$, against deviator stress, $q=\sigma_a-\sigma_o$, as shown in Fig. 4(c). It is seen in Fig. 4(c) that starting from the initial net stress of $\sigma_{no}=50$ kPa, the net stress σ_n gradually reduces during undrained cyclic excitation and the stress path eventually touches upon the failure envelope on the extension side. It is at this point that the rapid increase of axial strain is initiated towards extension, as clearly shown in the plots of axial strain ε_a against deviator stress q in Fig. 4(d). Herein, in Fig. 4(d), the volume contraction and axial compression take positive values and the volume dilation and axial extension take negative values.

The same set of diagrams is shown in Fig. 5 for one of the test results on Urayasu sand with $D_r=70\%$ and $S_r=67\%$ conducted under $\sigma_d/(2\sigma_{no})=0.51$. The responses of pore air and pore water pressures against cyclic excitation can be clearly seen in Fig. 5(a), though the significant increase of pore pressures seem not induced for Urayasu sand. On the other hand, it is seen in Fig. 5(b) that the development of axial strain ε_a tends to deviate towards extension significantly, leaving the development of volumetric strain ε_v almost equal to none on average. It appears from those data that since no significant residual volumetric strain develops for Urayasu sand, little development occurred with regard to residual pore air and pore water pressures. Without any significant developments in the pore air and pore water pressures during undrained cyclic excitation, the net stress would not reduce significantly, though the stress path begins to touch upon the failure envelope on the extension side under such a large value of the cyclic stress ratio, and the axial strain starts to develop progressively, as shown in Fig. 5(c) and (d).

4.2. Evaluation of soil liquefaction triggering and cyclic resistance

Soil liquefaction triggering has long been one of the primary concerns for geotechnical engineering, though the consequence of soil liquefaction tends to cause more social and practical concerns. In estimating triggering of soil liquefaction for saturated sands, the pore water pressure buildup is one of the clear indications.

There are several ways to look at the triggering of soil liquefaction for unsaturated soils. Based on the data shown in Figs. 4 and 5, the most comprehensible way is to look at the reduction of net stress, $\sigma_n=\sigma_o-u_a$, though it is also necessary to pay due attention to the change in the matric suction, $S_u=u_a-u_w$.

It was also demonstrated by Unno et al. (2008) that the development of volumetric strain can be used for estimating soil liquefaction triggering for unsaturated soils. Where it is possible to assume that the entire volume of pore air within a soil specimen could diminish, the maximum value of

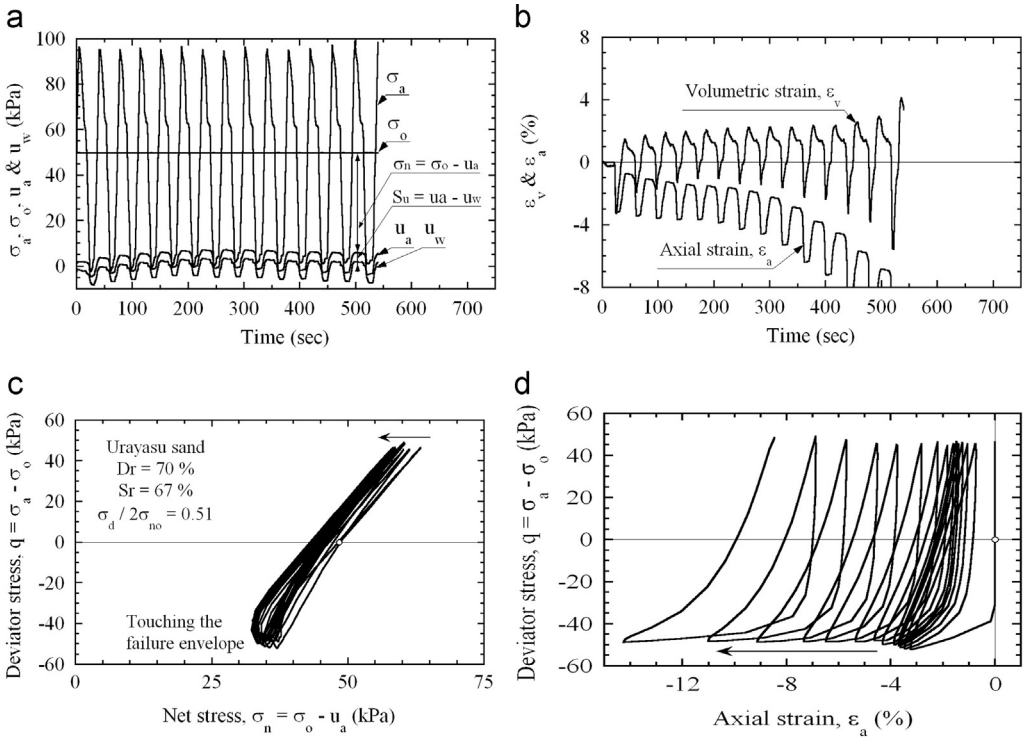

Fig. 5. Typical test results, (a) σ_a, σ_o, u_a & u_w – time, (b) ε_v & ε_a – time, (c) $q-\sigma_n$, (d) $q-\varepsilon_a$, (Urayasu sand, $D_r=70\%$, $S_r=67\%$, $\sigma_d/2\sigma_{no}=0.51$).

Please cite this article as: Tsukamoto, Y., et al., Cyclic resistance of two unsaturated silty sands against soil liquefaction. Soils and Foundations (2014), http://dx.doi.org/10.1016/j.sandf.2014.11.005

volumetric strain $\varepsilon_{v,a}$ is given as follows:

$$\varepsilon_{v,a} = \frac{e(1-Sr)}{1+e} \quad (1)$$

where e is the void ratio and S_r is the degree of saturation. However, it was assumed by Unno et al. (2008) that at the onset of soil liquefaction for unsaturated soils, the pore air pressure rises and becomes equal to the confining stress, leading to the following equilibrium equation:

$$u_{ao\_abs} \times V_{ao} = \sigma_{o\_abs} \times (V_{ao} - \Delta V_a) \quad (2)$$

where V_{ao} is the initial volume occupied by pore air and ΔV_a is the volume change of unsaturated soil structures, while u_{ao_abs} and σ_{o_abs} are the initial pore air pressure and the confining stress, defined both in absolute pressures. By introducing the relations of $\varepsilon_{v,l} = \Delta V_a / V_o$ and $V_{ao}/V_o = e(1-Sr)/(1+e)$, the above equation is rewritten and the liquefaction-inducing volumetric strain $\varepsilon_{v,l}$ can be determined as follows:

$$\varepsilon_{v,l} = \left(1 - \frac{u_{ao\_abs}}{\sigma_{o\_abs}}\right) \times \frac{e(1-Sr)}{1+e} = \left(1 - \frac{u_{ao\_abs}}{\sigma_{o\_abs}}\right) \times \varepsilon_{v,a} \quad (3)$$

In the present study, the triaxial tests are conducted with $u_{ao}=0$ kPa and $\sigma_o=50$ kPa in gauge pressures. Therefore, the relation of $\varepsilon_{v,l}=\varepsilon_{v,a}/3$ holds.

There is another issue associated with defining soil liquefaction triggering for unsaturated soils. In undrained cyclic tests on fully saturated sands, the full development of excess pore water pressure reaching the level of initial effective confining stress, in other words, the zero effective stress is considered as onset of soil liquefaction. The development of axial strain ε_a would solely correspond to the development of shear strain γ and would not cause any development of volumetric strain ε_v. The double amplitude axial strain of DAε_a=5% is then used to determine the number of cycles necessary to cause soil liquefaction, which is equivalent to the double amplitude of shear strain of DAγ=7.5%, since the shear strain is defined as $\gamma=\varepsilon_a-\varepsilon_h$ and no volumetric strain is induced, $\varepsilon_v=\varepsilon_a+2\varepsilon_h=0$, where ε_h is the lateral strain. On the other hand, in case of unsaturated sands, the development of excess pore water and pore air pressures reaching the level of initial effective confining stress was also used to categorise the occurrence of liquefaction in unsaturated sand, (Unno et al., 2008). In case of unsaturated sands, the development of axial strain ε_a would contribute to the developments of shear strain γ as well as volumetric strain ε_v. The developments of shear strain as well as volumetric strain would surely contribute to the developments of excess pore water and pore air pressures. From the viewpoint of characterizing soil liquefaction triggering in terms of strain developments, one of the conceivable procedures is to use directly the value of DAγ=7.5%, instead of using DAε_a=5%, by calculating the development of shear strain according to the expression as follows:

$$\gamma = \frac{3}{2}\varepsilon_a - \frac{1}{2}\varepsilon_v \quad (4)$$

However, this procedure does not take the effects of volumetric strain into account, and was found to give rise to far larger numbers of cycles necessary to induce DAγ=7.5%, leading to highly unconservative values of cyclic resistance for unsaturated soils. In the present study, DAε_a=5% is simply used to determine the number of cycles necessary to cause soil liquefaction. The value of cyclic stress ratio, $\sigma_d/(2\sigma_{no})$, necessary to cause DAε_a=5% at a number of cycles of $N_c=20$ is then defined as the cyclic resistance ratio $\sigma_{d,l}/(2\sigma_{no})$.

4.3. Net stress reduction and suction

Fig. 6 shows the plots of net stress reduction ratio against the initial degree of saturation for Inagi sand. Herein, the net stress reduction ratio r_n is defined as follows:

$$r_n = \frac{\sigma_n}{\sigma_{no}} \quad (5)$$

The value of r_{n5} is determined as the net stress reduction ratio, observed at DAε_a=5%, and is extracted from the test results in the present study. It is seen in Fig. 6 that the net stress substantially reduces with increasing initial degree of saturation S_{ri}, however, it seems to have not reached the level required to trigger soil liquefaction, at least not in the tested range of S_r=40% to 70%. It is also necessary to look at the other component of stress state variables, the matric suction, which was described above. The values of initial suction and suction observed at DAε_a=5%, S_{uo} and S_{u5}, are plotted against degree of saturation S_r, as shown in Fig. 7. Herein, the values of S_r at DAε_a=5% are assumed to correspond to the residual degree of saturation attained after undrained cyclic excitation, and are therefore calculated by assuming the average values of volumetric strain ε_{v5}. There appear to be no significant changes

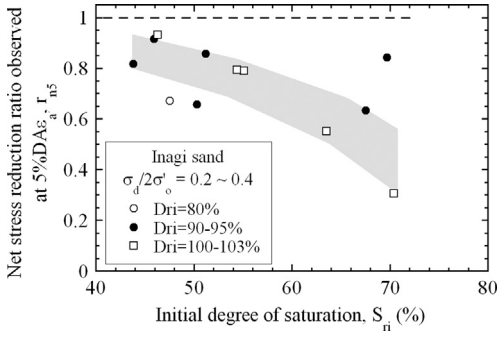

Fig. 6. Plots of Net stress reduction ratio observed at 5%DAε_a, r_{n5}, against initial degree of saturation S_{ri}, (Inagi sand).

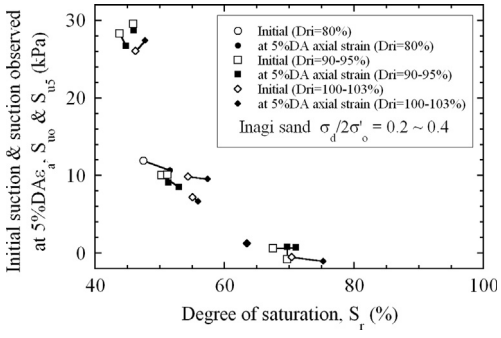

Fig. 7. Plots of initial suction and suction observed at 5%DAε_a, S_{uo} & S_{u5}, against degree of saturation S_r, (Inagi sand).

Please cite this article as: Tsukamoto, Y., et al., Cyclic resistance of two unsaturated silty sands against soil liquefaction. Soils and Foundations (2014), http://dx.doi.org/10.1016/j.sandf.2014.11.005

in the suction, while the changes in the degree of saturation seem more pronounced.

Figs. 8 and 9 show the same set of diagrams for Urayasu sand. The values of net stress reduction ratio are found to stay high in the range of S_r=40% to 70% tested. This is expected from the detailed look at the results of Urayasu sand shown in Fig. 5, as described above. It is also interesting to see that the values of suction induced in Urayasu sand are very low. This seems to contradict the fact that Urayasu sand contains more fines of less than 0.075 mm than Inagi sand. However, in terms of D_{10} values, Inagi sand has a far smaller value than Urayasu sand, as shown in Table 1. There have been some past studies examining the capillary effects on the small-strain modulus of unsaturated soils in relation to D_{10} values, (Wu et al., 1984 and others). Nevertheless, with only a limited number of data on the two silty sands, it would be inappropriate to extend the discussions to what the most relevant index parameters to reflect the extent of suction development within soil structures would be.

4.4. Volumetric strain

Fig. 10 shows the plots of volumetric strain observed at DAε_a,=5%, ε_{v5}, against the initial degree of saturation S_{ri} for Inagi sand. Since the observed volumetric train oscillates during undrained cyclic excitation as shown in Fig. 4(b), the maximum, average and minimum values are plotted. In some of the tests, the observed axial strain has not reached DAε_a,=5%. In such cases, the values of volumetric strain

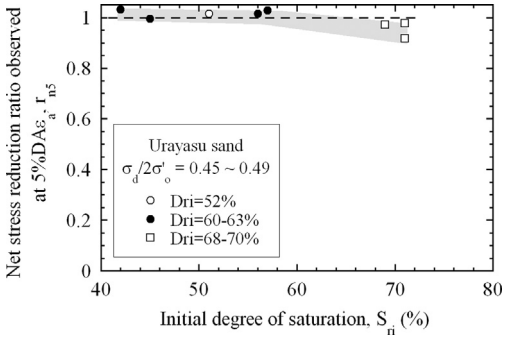

Fig. 8. Plots of Net stress reduction ratio observed at 5%DAε_a, r_{n5}, against initial degree of saturation S_{ri}, (Urayasu sand).

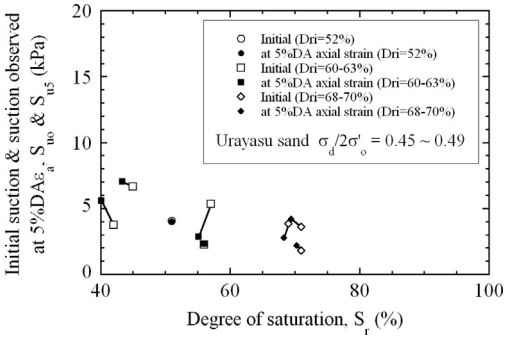

Fig. 9. Plots of initial suction and suction observed at 5%DAε_a, S_{uo} & S_{u5}, against degree of saturation S_r, (Urayasu sand).

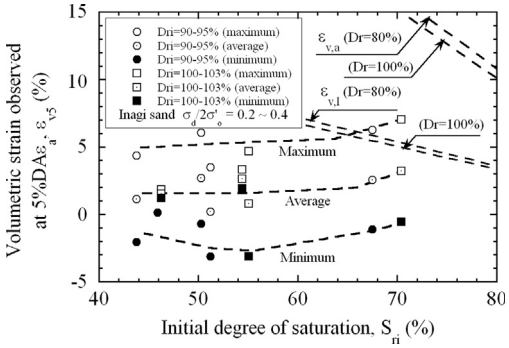

Fig. 10. Plots of volumetric strain observed at 5% DAε_a, ε_{v5}, against initial degree of saturation S_{ri}, (Inagi sand).

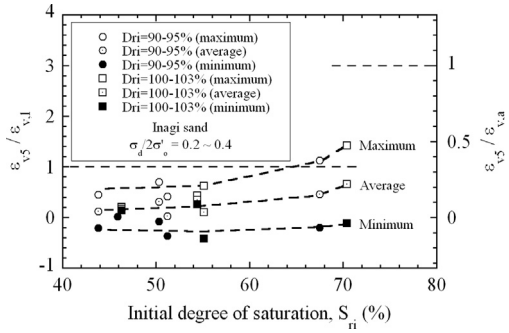

Fig. 11. Plots of volumetric strain ratios, $\varepsilon_{v5}/\varepsilon_{v,l}$ & $\varepsilon_{v5}/\varepsilon_{v,a}$, against initial degree of saturation S_{ri}, (Inagi sand).

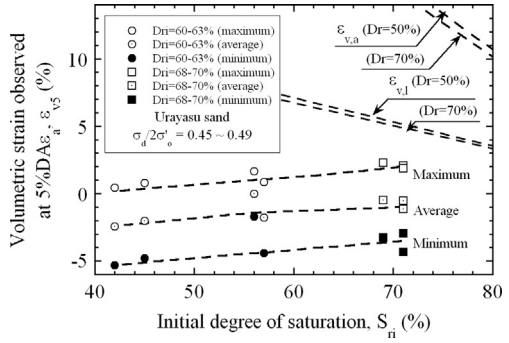

Fig. 12. Plots of volumetric strain observed at 5% DAε_a, ε_{v5}, against initial degree of saturation S_{ri}, (Urayasu sand).

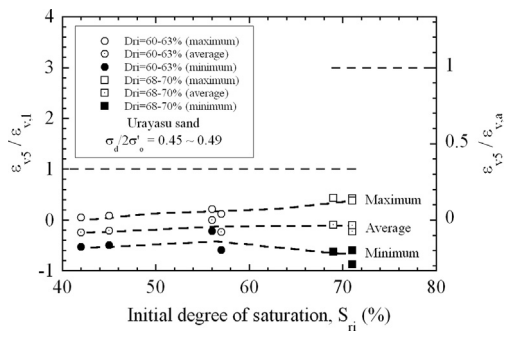

Fig. 13. Plots of volumetric strain ratios, $\varepsilon_{v5}/\varepsilon_{v,l}$ & $\varepsilon_{v5}/\varepsilon_{v,a}$, against initial degree of saturation S_{ri}, (Urayasu sand).

Please cite this article as: Tsukamoto, Y., et al., Cyclic resistance of two unsaturated silty sands against soil liquefaction. Soils and Foundations (2014), http://dx.doi.org/10.1016/j.sandf.2014.11.005

are picked up from the last cycle of undrained cyclic excitation. In Fig. 10, the threshold lines for the two limiting volumetric strains of $\varepsilon_{v,l}$ and $\varepsilon_{v,a}$ are also indicated. The maximum values of volumetric strain of ε_{v5} tend to exceed the limiting liquefaction-triggering volumetric strain of $\varepsilon_{v,l}$ at around S_{ri}=70%. However, they stay far below the other limiting volumetric strain of $\varepsilon_{v,a}$. This is clearly seen in Fig. 11, where the ratios of ε_{v5} /$\varepsilon_{v,l}$ and ε_{v5} /$\varepsilon_{v,a}$ are plotted against the initial degree of saturation S_{ri}. Figs. 12 and 13 show the same set of diagrams for Urayasu sand. All the observed values of volumetric strain of ε_{v5} stay well below the threshold lines of $\varepsilon_{v,l}$, implying it is unlikely that soil liquefaction triggering will be observed in the range of S_r=40 to 70% tested for Urayasu sand. This is consistent with the behaviour of net stress reduction ratio examined above. This difference in the volume contraction characteristics of the two unsaturated silty sands is likely to arise from the fact that the observed axial strain of Urayasu sand tends to deviate towards extension more progressively than that of Inagi sand, as shown in Figs. 4 and 5.

From the overall look at the results of net stress reduction ratio and volumetric strain as described above, it is unlikely that soil liquefaction is triggered in the range of degree of saturation less than S_r=70%. It is therefore appropriate to estimate that the degree of saturation larger than S_r=70% necessary for soil liquefaction triggering even for silty sands. However, in the present study the aim is to examine the overall relation between cyclic resistance and degree of saturation, and is not particularly intended to pursue a more detailed account of what occurs in the range larger than S_r=70%.

4.5. Cyclic resistance

From the results of some of the unsaturated cyclic triaxial test series, the values of cyclic stress ratios, σ_d / $2\sigma_{no}$, to cause DAε_a=5% are plotted against number of cycles, N_c, for Inagi sand and Urayasu sand, as shown in Figs. 14 and 15. In some of the tests shown in Figs. 14 and 15, the axial strain was not developed to achieve DAε_a=5%. In such cases, the data points are included with the values of DAε_a achieved. The cyclic

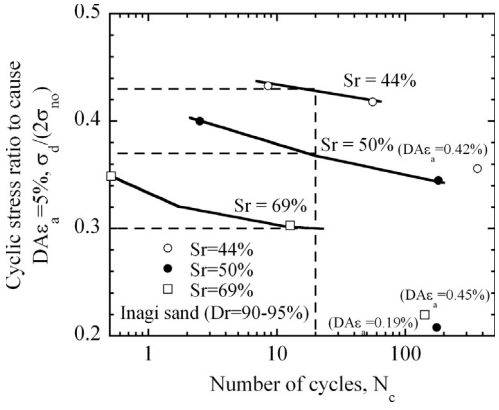

Fig. 14. Plots of cyclic stress ratios, σ_d / $2\sigma_{no}$, to cause DAε_a=5% against number of cycles, N_c, (Inagi sand).

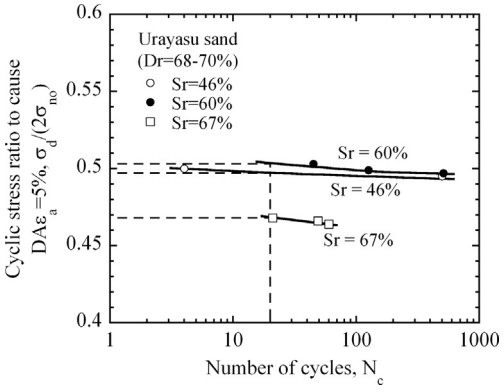

Fig. 15. Plots of cyclic stress ratios, σ_d / $2\sigma_{no}$, to cause DAε_a=5% against number of cycles, N_c, (Urayasu sand).

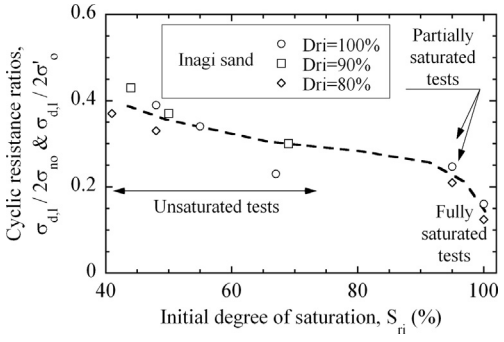

Fig. 16. Plots of cyclic resistance ratios, $\sigma_{d,l}$ / $2\sigma_{no}$ & $\sigma_{d,l}$ / $2\sigma'_o$, against initial degree of saturation S_{ri}, (Inagi sand).

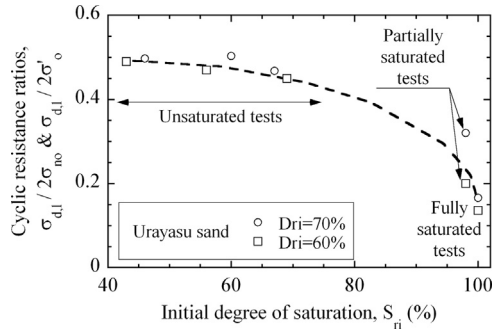

Fig. 17. Plots of cyclic resistance ratios, $\sigma_{d,l}$ / $2\sigma_{no}$ & $\sigma_{d,l}$ / $2\sigma'_o$, against initial degree of saturation S_{ri}, (Urayasu sand).

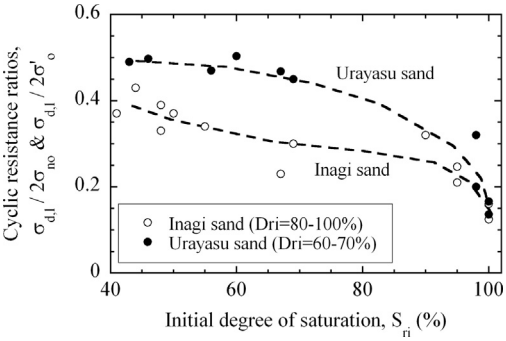

Fig. 18. Comparison of cyclic resistance ratios and S_{ri} relations for Inagi sand and Urayasu sand.

Please cite this article as: Tsukamoto, Y., et al., Cyclic resistance of two unsaturated silty sands against soil liquefaction. Soils and Foundations (2014), http://dx.doi.org/10.1016/j.sandf.2014.11.005

resistance ratios are then determined as the cyclic stress ratios corresponding to the number of cycles, N_c=20.

Fig. 16 shows the plots of cyclic resistance ratios of $\sigma_{d,l}/(2\sigma_{no})$ and $\sigma_{d,l}/(2\sigma'_o)$ against initial degree of saturation S_{ri} for Inagi sand. Herein, the cyclic resistance ratio of $\sigma_{d,l}/(2\sigma_{no})$ is defined for unsaturated soil tests, while $\sigma_{d,l}/(2\sigma'_o)$ is defined for partially and fully saturated soil tests. Cyclic resistance is found to reduce gradually with increasing degree of saturation, and tends to reduce rapidly when the value of S_r reaches about 95%. The same plots for Urayasu sand are shown in Fig. 17. The cyclic resistance tends to stay high to a value of S_r=70%, and then tends to reduce gradually with increasing degree of saturation. The relations of cyclic resistance ratios and S_{ri} for Inagi sand and Urayasu sand are compared as shown in Fig. 18. The cyclic resistance of Urayasu sand is found generally larger than that of Inagi sand. This seems to be consistent with the difference in the behaviour of net stress reduction ratio and volumetric strain examined above. The difference in the cyclic resistance of the two silty sands is therefore strongly associated with the volume change characteristics during undrained cyclic excitation, resulting in the difference in the developments of pore air and pore water pressures. It is therefore appropriate to mention that those two silty sands with different grain size compositions exhibited different behaviours during undrained cyclic excitation, leading to different relations between the cyclic resistance and degree of saturation, though the cyclic resistance at unsaturated conditions is found to be remarkably larger than that at fully saturated conditions.

5. Conclusions

Multiple series of undrained cyclic triaxial tests were conducted on two silty sands under unsaturated, partially saturated and fully saturated conditions. The relationships between the cyclic resistance and degree of saturation were obtained for the two silty sands, and were discussed in relation to the net stress reduction and volumetric strain development. The two silty sands with different grain size compositions gave rise to different volume change characteristics during undrained cyclic excitation, resulting in a difference in the developments of pore air and pore water pressures. This led to a difference in the relationship between the cyclic resistance and the degree of saturation for the two silty sands.

Acknowledgements

The laboratory triaxial tests described in the present study were conducted with a help of past students of Tokyo university of Science, K. Imori, M. Inami, M. Ishii, K. Oizumi, A. Suzuki, M. Yokoyama. The authors are grateful to their cooperation.

References

Chiaro, G., Koseki, J., Sato, T., 2012. Effects of initial static shear on liquefaction and large deformation properties of loose saturated Toyoura sand in undrained cyclic torsional shear tests. Soils and Foundations 52 (3), 498–510.

Chiaro, G., Kiyota, T., Koseki, J., 2013. Strain localization characteristics of loose saturated Toyoura sand in undrained cyclic torsional shear tests with initial static shear. Soils and Foundations 53 (1), 23–34.

Fredlund, D.G., Rahardjo, H., 1993. Soil mechanics for unsaturated soils. A Wiley-Interscience Publication, John Wiley & Sons, New York.

Grozic, J.L.H., Robertson, P.K., Morgenstern, N.R., 1999. The behavior of loose gassy sand. Canadian Geotechnical Journal 36, 482–492.

Grozic, J.L.H., Robertson, P.K., Morgenstern, N.R., 2000. Cyclic liquefaction of loose gassy sand. Canadian Geotechnical Journal 37, 843–856.

Higo, Y., Oka, F., Sato, T., Matsushima, Y., Kimoto, S., 2013. Investigation of localized deformation in partially saturated sand under triaxial compression. Soils and Foundations 53 (2), 181–198.

Ishihara, K., Tsukamoto, Y., 2004. Cyclic strength of imperfectly saturated sands and analysis of liquefaction. Proceedings of the Japan Academy, Ser. B Vol.80 (No.8), 372–391.

Ishihara, K., Tsukamoto, Y., Kamada, K., 2004. Undrained behaviour of near-saturated sand in cyclic and monotonic loading, Proceedings of International Conference on Cyclic Behaviour of Soils and Liquefaction Phenomena, Bochum, Germany, 31 March – 02 April 2004; Cyclic Behaviour of Soils and Liquefaction Phenomena (ed. Th. Triantafyllidis), 27–39. Taylor & Francis Group, London.

Ishikawa, T., Zhang, Y., Tokoro, T., Miura, S., 2014. Medium-size triaxial apparatus for unsaturated granular subbase course materials. Soils and Foundations 54 (1), 67–80.

Japanese Geotechnical Society, 2009. Test methods for minimum and maximum densities of soils. Geotechnical Testing Standards, 195–225 (in Japanese).

Kamata, T., Tsukamoto, Y., Tatsuoka, F. and Ishihara, K. (2007): Possibility of undrained flow in unsaturated sandy soils in triaxial tests, Proceedings of 4th International Conference on Earthquake Geotechnical Engineering, Thessaloniki, Greece, June 25-28, 2007, Paper No. 1289.

Kamata, T., Tsukamoto, Y., Ishihara, K., 2009. Undrained shear strength of partially saturated sand in triaxial tests. Bulletin of the New Zealand Society for Earthquake Engineering 42 (1), 57–62.

Sawada, S., Tsukamoto, Y., Ishihara, K., 2006. Residual deformation characteristics of partially saturated sandy soils subjected to seismic excitation. Soil Dynamics and Earthquake Engineering 26, 175–182.

Tsukamoto, Y., Ishihara, K., Nakazawa, H., Kamada, K., Huang, Y., 2002. Resistance of partly saturated sand to liquefaction with reference to longitudinal and shear wave velocities. Soils and Foundations 42 (6), 93–104.

Unno, T., Kazama, M., Uzuoka, R., Sento, N., 2008. Liquefaction of unsaturated sand considering the pore air pressure and volume compressibility of the soil particle skeleton. Soils and Foundations 48 (1), 87–99.

Wu, S., Gray, D.H., Richart Jr., F.E., 1984. Capillary effects on dynamic modulus of sands and silts. Journal of Geotechnical Engineering, ASCE 110 (9), 1188–1203.

Yang, J., 2002. Liquefaction resistance of sand in relation to P-wave velocity. Geotechnique 52 (4), 295–298.

Yang, J., 2004. Evaluating liquefaction strength of partially saturated sand. Journal of Geotechnical and Geoenvironmental Engineering, ASCE 130 (9), 975–979.

Please cite this article as: Tsukamoto, Y., et al., Cyclic resistance of two unsaturated silty sands against soil liquefaction. Soils and Foundations (2014), http://dx.doi.org/10.1016/j.sandf.2014.11.005